Supporting Information

External forcing explains recent decadal variability of the ocean carbon sink

Galen A. McKinley[1], Amanda R. Fay[1], Yassir A. Eddebbar[2], Lucas Gloege[1],
Nicole S. Lovenduski[3]

[1] Lamont Doherty Earth Observatory / Columbia University, Palisades NY
[2] Scripps Institution of Oceanography, La Jolla, CA
[3] University of Colorado at Boulder, Boulder, CO

Models and Products

In addition to the 6 hindcast models used throughout this analysis, nine (9) hindcast model-based estimates of the effect of constant climate and variable $pCO_2^{atmosphere}$ for 1980-2016 are used to provide a comparison to other recent work (Devries et al. 2019; Figure 1b). Of the 9 models in this suite, 6 are essentially the same as those in our primary analysis. Correlation of the mean of this 9-member ensemble with variable climate and variable $pCO_2^{atmosphere}$ for 1980-2016 (Devries et al. 2019) to our suite of hindcast models is 0.99, indicating that the results are interchangeable for the purpose of this paper.

Flux analysis

Individual models and products utilize different methods for flux calculation including wind speed products and parameterizations. References included in Table S1 and Table S2 provide details on each model and product.

pCO$_2$ analysis

For both models and products, maps of flux indicate that ice coverage has been considered in the calculation, however spatially-resolved pCO_2 do not indicate this masking. Therefore, we begin by accounting for ice coverage in the pCO_2 analysis for each model and product [$pCO_2^{ocean} = pCO_2^{ocean, raw} *(1\text{-ice fraction})$] with ice fraction product NOAA_OI_SST_V2. These data provided by the NOAA/OAR/ESRL PSD, Boulder, Colorado USA from their website at https://www.esrl.noaa.gov/psd/ (Reynolds et al., 2002). The ice fraction product begins in 1982. In order to apply it to models that begin in 1980, we use the 1982-1989 monthly climatology for 1980 and 1981.

ΔpCO_2 is calculated at annual timescales by [$\Delta pCO_2 = pCO_2^{ocean} - pCO_2^{atmosphere}$] where $pCO_2^{atmosphere}$ is the dry air mixing ratio of atmospheric CO_2 (xCO_2) from the ESRL surface marine boundary layer CO_2 product available at https://www.esrl.noaa.gov/gmd/ccgg/mbl/data.php (Dlugokencky et al., 2017) and sea level pressure (Kalnay et al., 1996) at monthly resolution. NCEP Reanalysis Derived data provided by the NOAA/OAR/ESRL PSD, Boulder, Colorado, USA, from their web site at https://www.esrl.noaa.gov/psd/. A global area-weighted annual time series is then calculated for $pCO_2^{atmosphere}$ before calculating ΔpCO_2.

Upper Ocean Box Model, Additional Discussion

The mean and standard deviation of the air-sea CO_2 flux in the box model is not very sensitive to reasonable parameter choices. Across the observed k_w range of 12-18 cm/hr (Wanninkhof, 2014), and reasonable estimates for the rate of overturning circulation (v) from 15-35 Sv (DeVries et al., 2017), the mean flux is not sensitive (Fig S3a); instead ΔpCO_2 adjusts such that the flux drives surface ocean pCO_2 so that it can, on the long-term, rise at the same rate as $pCO_2^{atmosphere}$ (Fig S6). The depth of the box does impact the mean flux (Fig S3b,c) because this alters the total volume of low carbon water supplied from depth that needs to equilibrate toward the rising $pCO_2^{atmosphere}$. The magnitude of variability ranges by approximately 20% across k_w values, but is not sensitive

53   to v. As the depth of the box becomes shallower than 400m, variability of the flux declines by up
54   to 25%. This sensitivity analysis indicates that our parameter choices do not dramatically influence
55   our results. In addition, our choice of parameters is supported by the fact that the box model forced
56   with only $pCO_2^{atmosphere}$ can capture air-sea CO_2 flux variability that is essentially identical to the
57   ensemble result from constant climate three-dimensional ocean models (Fig. 1b).
58

59   When the box model is forced with only the 1980-2017 linear change of $pCO_2^{atmosphere}$ (1.78
60   µatm/yr) (Fig S6a,d), the response is an increased carbon flux into the ocean until the point that a
61   new approximately steady-state ΔpCO_2 is achieved (Fig S6e). This ΔpCO_2 provides sufficient flux
62   for the annual growth of pCO_2^{ocean} to approximately match that of $pCO_2^{atmosphere}$, and thus there is
63   a steady carbon flux (Fay & McKinley, 2013; McKinley et al., 2017). The timescale for this
64   equilibration is approximately 10 years, calculated as 2 e-folding timescales for the adjustment to
65   a new steady state for the box model forced only with linear trend of $pCO_2^{atmosphere}$. Because there
66   are no short-term anomalies in either pCO_2^{ocean} or $pCO_2^{atmosphere}$ when forced with linear trend of
67    $pCO_2^{atmosphere}$, there is also no interannual variability of ΔpCO_2 (Fig S6f) or flux (not shown) in
68   this case. Adding the volcano SST forcing (Fig S2) the box model forced with linear trend of
69    $pCO_2^{atmosphere}$, there are immediate negative anomalies in ΔpCO_2, indicating an increased sink, and
70   then a relaxation as the surface ocean re-warms with the fading of the volcano cooling effect (Fig
71   S6e,f).
72

73   **Table S1: Hindcast model resolution and coverage period. Total ocean coverage is based on**
74   **the 1ºx1º mask of Gruber et al., 2009 used in the RECCAP project (Canadell et al., 2011).**
75

Model Name *Reference*	Resolution Years	Area Coverage (% global ocean)
MITgcm-REcoM2 *Hauck et al. 2018*	Monthly, 1°x1° 1958-2017	$3.51e+14 m^2$ (96%)
NEMO-PlankTOM *Buitenhuis et al. 2010*	Monthly, 1°x1° 1959-2017	$3.49e+14 m^2$ (96%)
CNRM-ESM2-1 *Séférian et al. 2016*	Monthly, 1°x1° 1848-2017	$3.61e+14 m^2$ (99%)
CCSM-BEC *Doney et al. 2009*	Monthly, 1°x1° 1958-2017	$3.29e+14 m^2$ (90%)
MPI-ESM *Paulsen et al. 2017*	Monthly, 1°x1° 1959-2017	$3.42e+14 m^2$ (94%)
NorESM-OCv1.2 *Schwinger et al. 2016*	Monthly, 1°x1° 1948-2017	$3.70e+14 m^2$ (101%)

76
77

78   **Table S2: Observationally-based product resolution and coverage period.** In the case of
79   time-varying coverage masks, area coverage listed is for a most conservative mask which
80   requires a value for every month of the time period. In some cases, this differs for flux and pCO_2
81   variables. Total ocean coverage is based on the 1x1º mask of Gruber et al., 2009 used in the
82   RECCAP project (Canadell et al., 2011).

83

Product Name *Reference*	Resolution Years	Area Coverage (% global ocean)	Mean Correction to Flux (to pCO_2) (section 2.4)
LSCE *Denvil-Sommer et al. 2019*	Monthly, 1°x1° 1985-2016	2.93e+14m² (80%)	0.41 PgCyr⁻¹ (3.18µatm)
CSIR-ML6 *Gregor et al. 2019*	Monthly, 1°x1° 1982-2016	Flux: 3.11e+14m² (85%) pCO_2: 3.13e+14 (86%)	0.30 PgCyr⁻¹ (1.98µatm)
SOM-FFN *Landschützer et al. 2017*	Monthly, 1°x1° 1982-2018	3.19e+14m² (87%)	0.25 PgCyr⁻¹ (1.56µatm)
Jena-MLS *Rödenbeck et al. 2013*	Monthly, 5°x5° 1982-2018 flux	3.67e+14m² (100%)	0

84
85

86   **Table S3: Parameters and values for the upper ocean diagnostic box model**

Parameter	Value	References / Notes
ν	25 Sv	Devries et al. 2017
DIC_{deep}	2055 mmol/m^3	Sarmiento and Gruber, 2006
k_w	15 cm/hr	Wanninkhof, 2014
Temperature	18°C	Sarmiento and Gruber, 2006
Salinity	35psu	
Alkalinity	2350 mmol/m^3	Sarmiento and Gruber, 2006
dz	500m	
Global ocean area (A)	3.34e14 m^2	96% of global ocean

87
88

89 **Table S4: Correlation of air-sea carbon flux for hindcast models, observationally-based**
90 **products, and box model runs as shown in Figure 1.** Detrended timeseries correlations shown
91 in parenthesis. Correlations are shown for longest overlapping timeseries. Correlations in bold
92 are significant at $p<0.05$.
93

	Hindcast models 1980-2017	Box Model 1980-2017	Hindcast models: $pCO_2{}^{atm}$ only 1980-2016	Box Model: $pCO_2{}^{atm}$ only 1980-2017	OCIM: $pCO_2{}^{atm}$ only 1980-2017
Observationally-based products 1985-2016	**0.95** **(0.78)**	**0.94** **(0.79)**	**0.86** (0.15)	**0.82** (0.17)	**0.87** (0.24)
Hindcast models 1980-2017	**1**	**0.92** **(0.64)**	**0.89** (-0.01)	**0.86** (0.02)	**0.90** (-0.01)
Box Model 1980-2017	-	**1**	**0.88** **(0.36)**	**0.90** **(0.46)**	**0.90** **(0.43)**
Hindcast models: $pCO_2{}^{atm}$ only 1980-2016	-	-	**1**	**0.98** **(0.93)**	**0.99** **(0.96)**
Box Model: $pCO_2{}^{atm}$ only 1980-2017	-	-	-	**1**	**0.98** **(0.85)**

94
95

96　**Table S5: Global Mean Fluxes (PgC/yr) by decade.** Observationally-based products have been
97　masked to account for missing ocean area.
98

Global Mean Flux (PgC/yr)	1980-1989	1990-1999	2000-2009	2010-2017
Box Model: actual $pCO_2{}^{atm}$ and volcano	-1.85	-1.97	-2.11	-2.48
Box Model: actual $pCO_2{}^{atm}$	-1.79	-1.88	-2.23	-2.50
Box Model: volcano only	-2.03	-2.31	-2.13	-2.20
Box Model: linear $pCO_2{}^{atm}$	-1.97	-2.22	-2.24	-2.22
Hindcast model mean	-1.68	-1.90	-2.05	-2.37
Observationally-based product mean	-1.42[a]	-1.62	-1.79	-2.38[b]

99　　a.　3 observationally-based products begin in 1982 and 1 in 1985 (Table S2)
100　　b.　Observationally-based products through 2016 only
101

$pCO_2^{atmosphere}$

air-sea flux

pCO_2^{ocean}

dz

overturning
circulation

102

103   **Figure S1: Schematic of the single-reservoir upper ocean diagnostic box model**
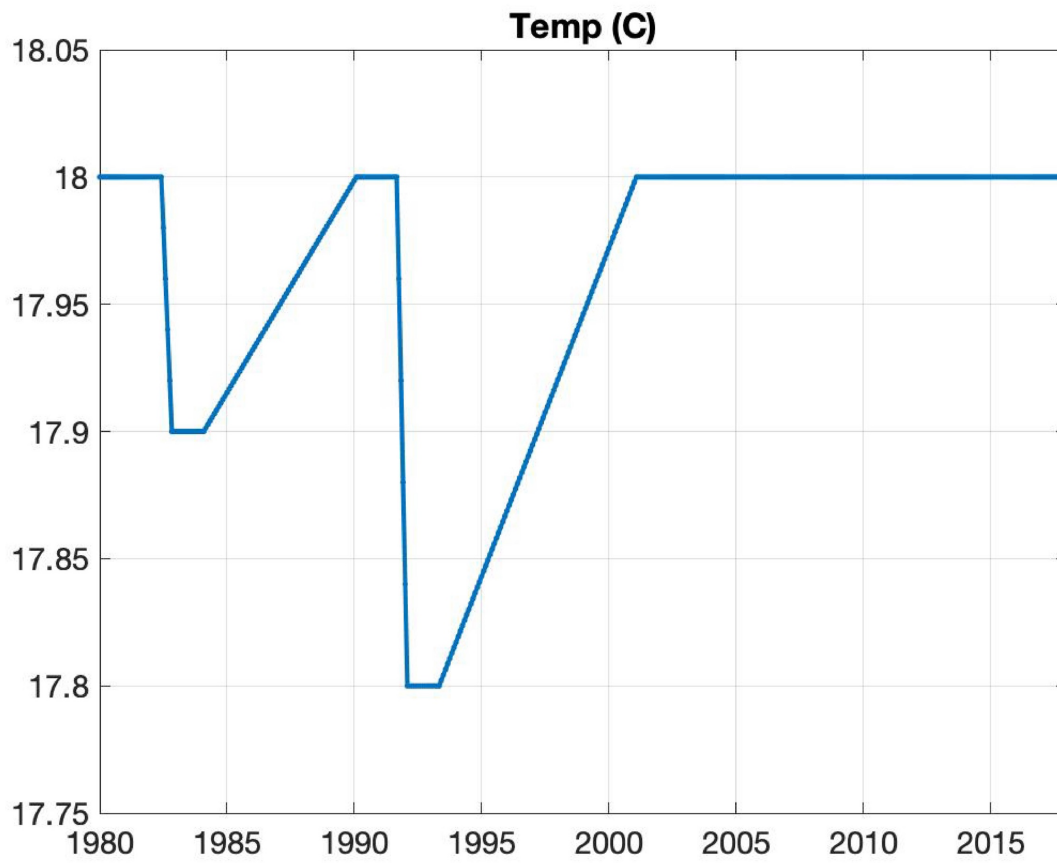
104

Figure S2: Sea surface temperature forcing for box model. Idealized SST response, based on two earth system models forced response to El Chichon and Mt. Pinatubo (Eddebbar et al. 2019, their Figure 1a)
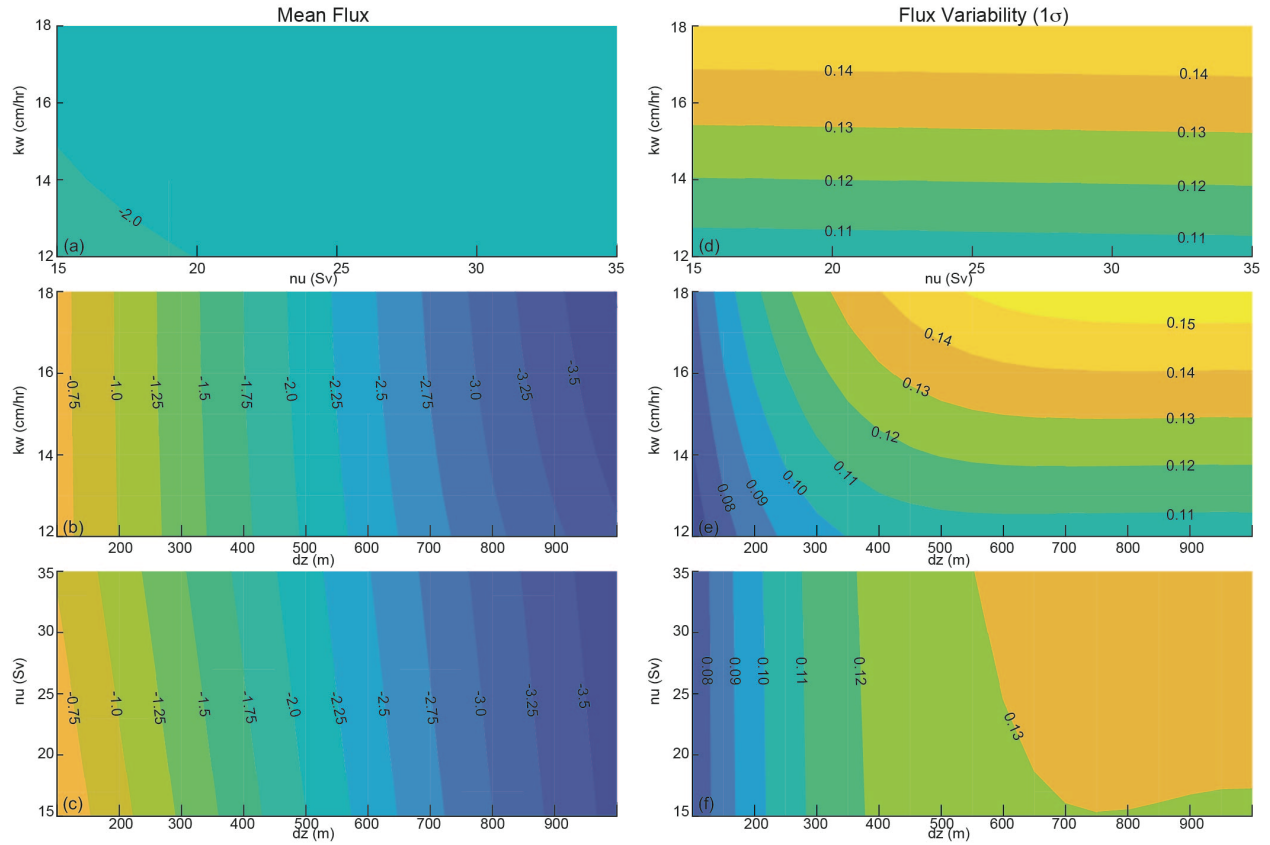
Figure S3: Sensitivity of the air-sea flux (PgC/yr) on the mean (a-c) and for variability (d-f) in the box model. The impact of varying values of piston velocity (k_w), the rate of the overturning circulation (ν), and the depth of the box (dz) on the box model forced with both $pCO_2{}^{atmosphere}$ and the SST response to volcanos. Default values are used for the third parameter in each case, e.g. (a,d) dz = 500m; (b,e), ν = 25 Sv; (c,f) k_w = 15 cm/hr.
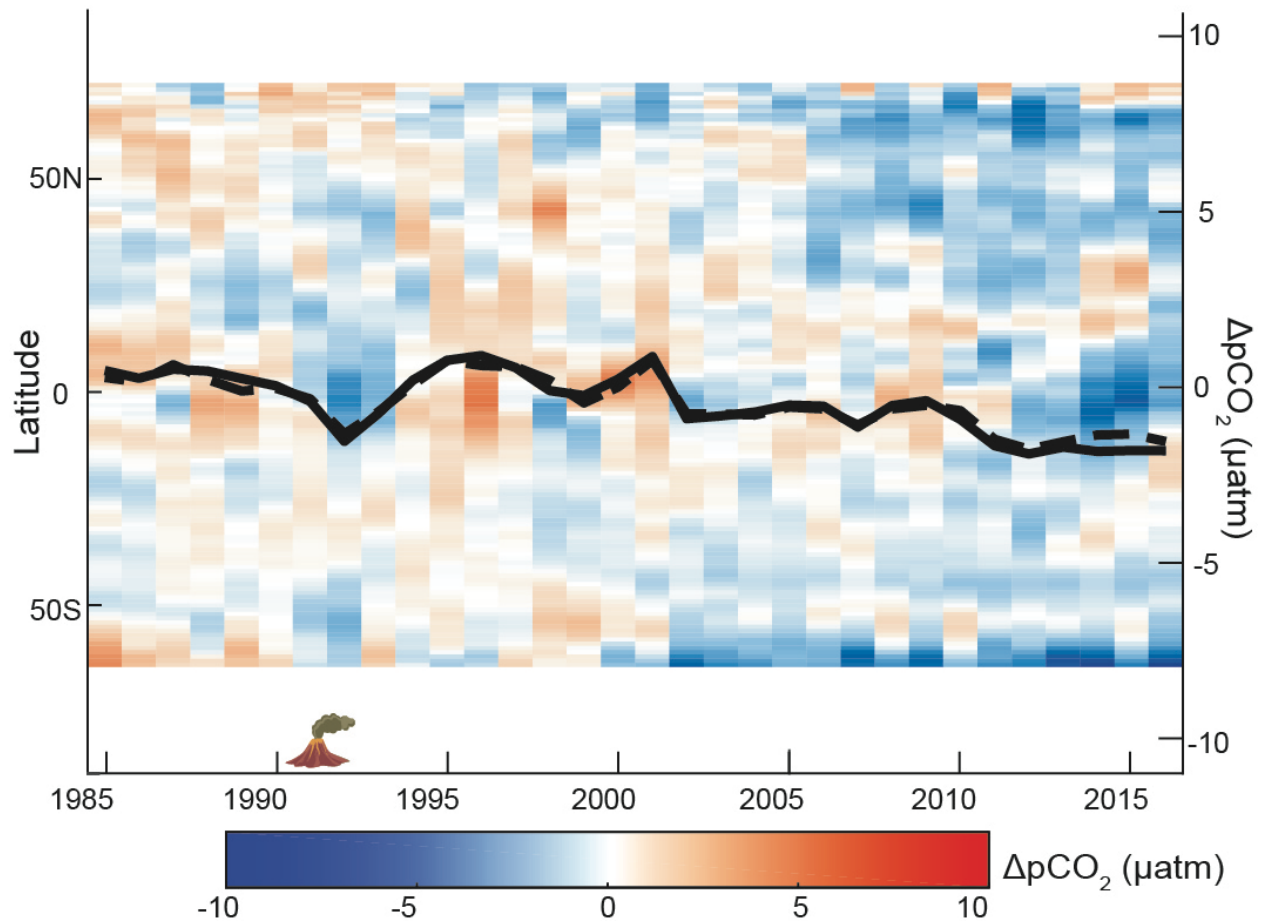
Figure S4: Latitudinal mean anomaly ΔpCO₂ (μatm) from the ensemble mean of the hindcast models. Anomaly is calculated from the 1990-1999 mean. Latitudes with >50% mean ice coverage omitted. Annual ΔpCO_2 time series overlaid in black for global (solid) and global excluding east equatorial Pacific biome (dashed).
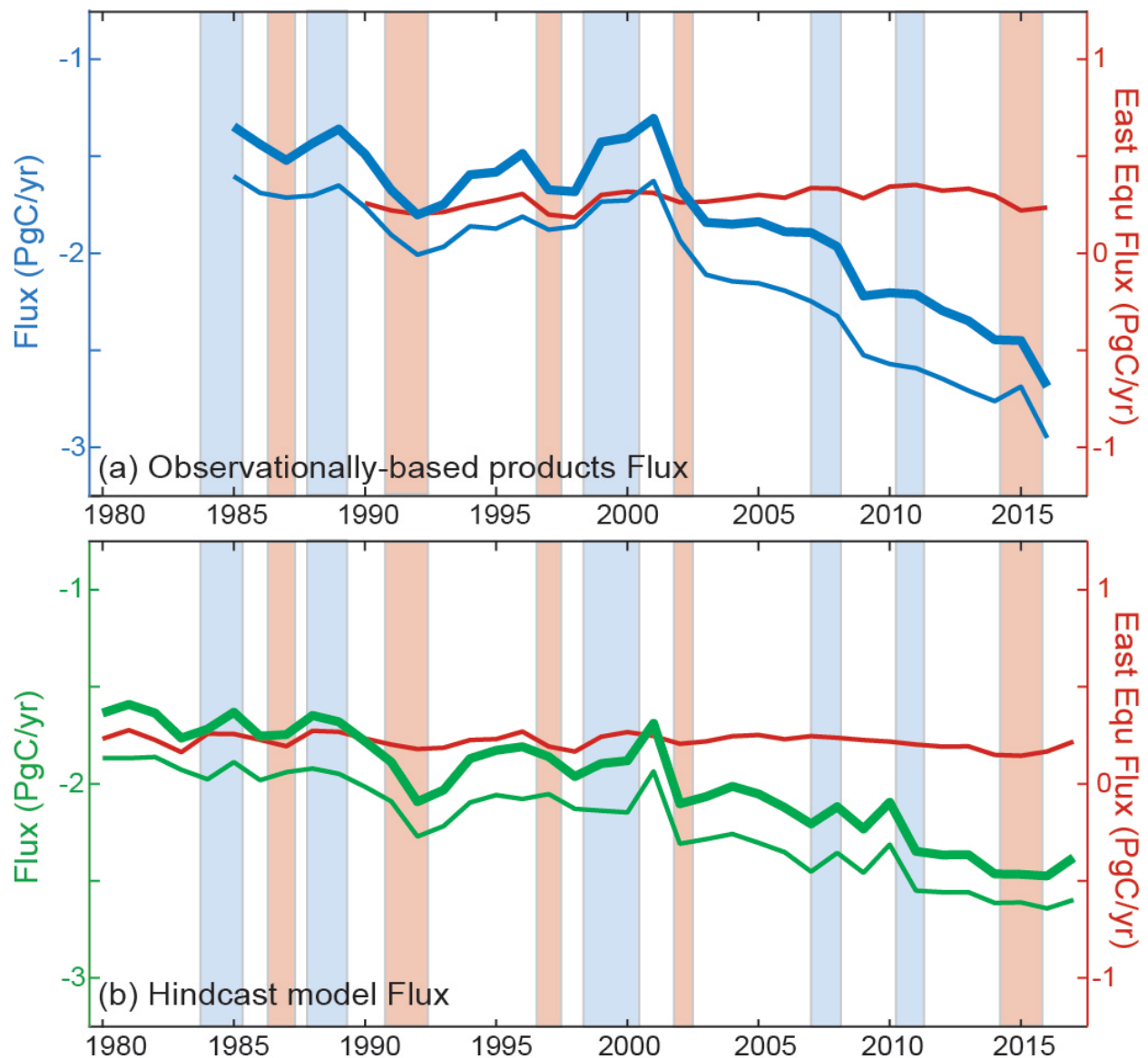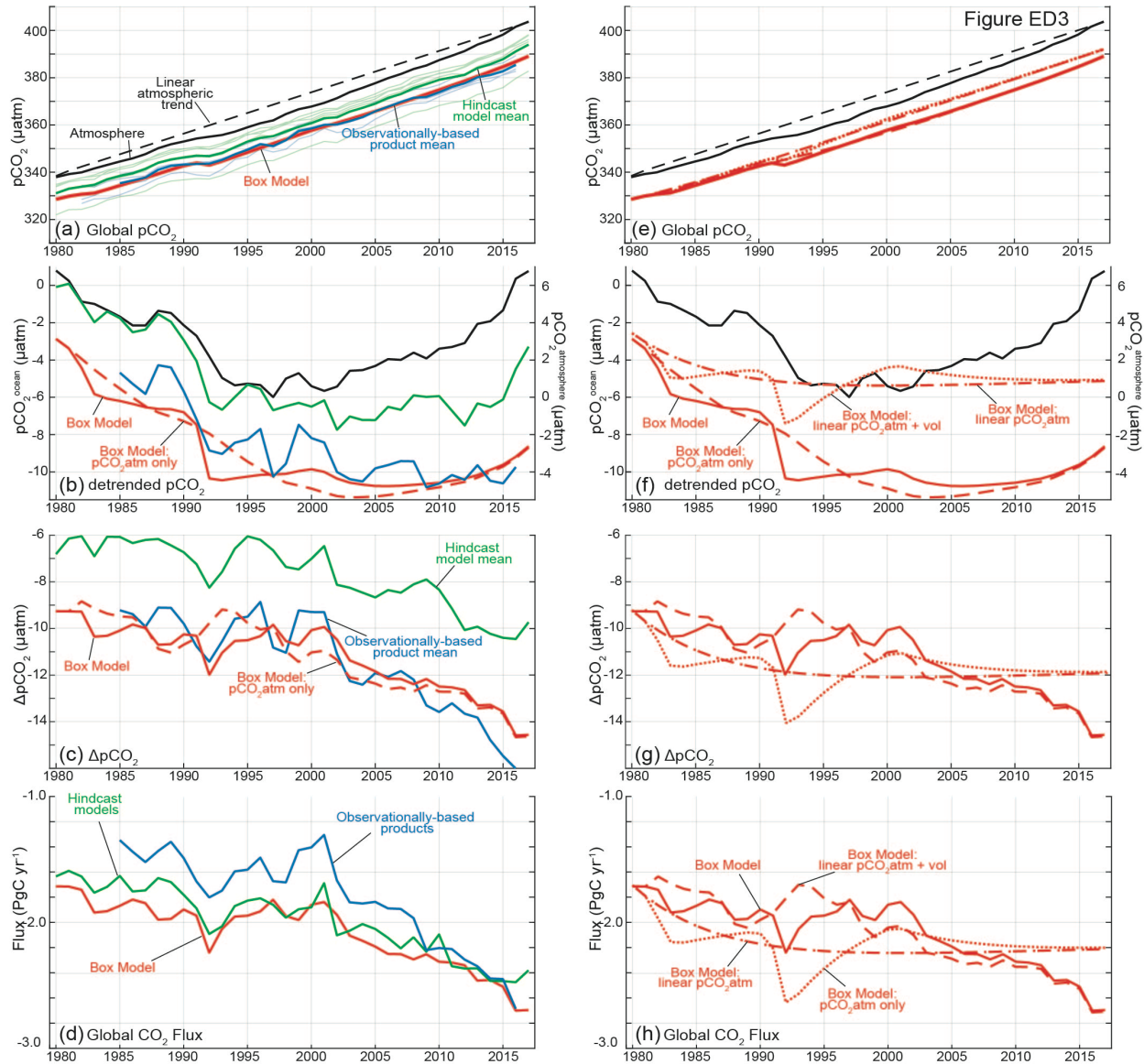
126

127
**Figure S5: Comparison of global fluxes and fluxes for the globe without the eastern
equatorial Pacific (Fay & McKinley 2014)**. (A) Observationally-based products (blue), (B)
hindcast models (green) for global (thick line), global without eastern equatorial Pacific biome
(thin line), and only east equatorial Pacific biome (red line). Shaded bars represent ENSO events;
blue for La Niña, red for El Niño. Though there is a high inverse correlation between CO_2 fluxes
and the Nino 3.4 index in the eastern equatorial Pacific ($r = -0.63$ for both products and models),
this region is small (4% of the global ocean area) and is not dominant to the global decadal flux
variability.

138

139
140

141 **Figure S6: Trends of pCO$_2^{atmosphere}$, pCO$_2^{ocean}$, and Air-sea CO$_2$ flux** (**A**) with trend, (**B**)
142 detrended with the long-change in pCO$_2^{atmosphere}$ (1.78 µatm/yr from 1980 to 2017), (**C**) ΔpCO$_2$
143 (= pCO$_2^{ocean}$ - pCO$_2^{atmosphere}$), and (**D**) global flux. Observationally-based products (blue),
144 hindcast models (green), upper ocean diagnostic box model (red). (**E**) Box model, 4 versions
145 with trend, (**F**) detrended with the long-term pCO$_2^{atmosphere}$ change (1.78 µatm/yr), (**G**) ΔpCO$_2$ (=
146 pCO$_2^{ocean}$ - pCO$_2^{atmosphere}$), and (**H**) global flux. E-H, the box model forced only with the linear
147 pCO$_2^{atmosphere}$ trend (dot-dash); with both linear pCO$_2^{atmosphere}$ trend and volcano SST (dotted);
148 with observed pCO$_2^{atmosphere}$ only (dash); and with observed pCO$_2^{atmosphere}$ and volcano SST
149 (solid).